Journal of Applied Sciences and Arts

Volume 1 | Issue 3 Article 4

December 2017

Comparison of New Metrics for Assessment of Risks of Occupational Noise

Wisam Al-Dayyeni
Southern Illinois University Carbondale, wisam.talib@siu.edu

Jun Qin
Southern Illinois University Carbondale, jqin@siu.edu

1 INTRODUCTION

Noise induced hearing loss (NIHL) remains as one of the most common occupational health problems in the world. According to the World Health Organization (WHO), exposure to excessive noise is the major avoidable cause of permanent hearing loss worldwide (Smith, 1996). There are over 500 million individuals at risk of developing NIHL worldwide (Sliwinska-Kowalska & Davis, 2012). In the United States, over 22 million workers were suffering from exposure to high-level noise which is loud enough to be potentially hazardous (Tak, Davis, & Calvert, 2009). Exposure to loud noise can cause serious damage to the hair cells inside the cochlea. The final result will be a permanent shift in the hearing threshold, known as NIHL.

Noises can be classified into continuous Gaussian noise (also called as steady-state noise), high-level transient noise (including impulse noise and impact noise), and complex noise (*i.e.*, a non-Gaussian noise consisting of high-level transients noise mixed in a Gaussian noise) (Hamernik, Qiu, & Davis, 2003b) (Hamernik, Qiu, & Davis, 2007) (Qin, Sun, & Walker, 2014) (Smalt, Lacirignola, Davis, Calamia, & Collins, 2017) (Wu & Qin, 2013). All types of noise could generate hearing loss at high noise intensity levels. A number of animal studies showed that complex noises can cause more hearing loss than continuous noise with the same energy level (Hamernik, Henderson, Crossley, & Salvi, 1974) (Blakeslee, Hynson, Hamernik, & Henderson, 1977) (Hamernik & Qiu, 2000) (Hamernik et al., 2003b) (Qin & Sun, 2015).

Various international standards have been developed to estimate NIHL, for example, CHABA (Smoorenburg, 1980), NOISH98 (Health & Services, 1998), MIL STD-1472F (AMSC & HFAC). These standards were designed based on either auditory weighting function (e.g., A-weighting) or based on the waveform empirical strategies (e.g., peak pressure and pulse duration) (Azizi, 2010) (Murphy & Kardous, 2012). In the current standards, the noise metrics are developed depending on the equal energy hypothesis (EEH), which states that NIHL mainly depends on the total acoustic energy of the exposure and it is independent on the temporal characteristics of that noise (Hamernik, Ahroon, Davis, & Lei, 1994) (Zhu, Kim, Song, Murphy, & Song, 2009). The primary metric to assess the exposure levels of the noise guideline is the A-weighted equivalent sound pressure level (SPL), L_{Aeq}. However, previous studies on NIHL indicated that L_{Aeq} is applicable for continuous noise (*i.e.*, Gaussian noise) but not for impact, impulsive or complex noises (Henderson & Hamernik, 1986) (Starck & Pekkarinen, 1987) (Hamernik et al., 1994) (Zhu et al., 2009) (Goley, Song, & Kim, 2011). Other studies also showed that the A-weighting filter is more appropriate to assess the low SPL, while the C-weighting filter is suitable for the high SPL (Parmanen,

2007). In addition, some researchers claimed that the EEH based metrics cannot provide a physical insight about NIHL, because they do not reflect the physical properties of the ear (Price, 2012).

To accurately evaluate high-level complex noise, we have recently developed new noise models for assessment of NIHL, including an adaptive weighting filter (F-weighting) (Sun, Qin, & Qiu, 2016) and the complex velocity level (CVL) auditory fatigue model (Sun & Qin, 2016) (Sun, Fox, Campbell, & Qin, 2017). In this study, we will further evaluate the performances of the newly developed F-weighting and CVL model based noise metrics using experimental noise exposure data on chinchilla, compared with conventional noise metrics (*i.e.*, A-weighted and C-weighted equivalent SPL).

2 METHODS AND MATERIALS

2.1 A-Weighting and C-Weighting

In the current standards, A-weighting is used to evaluate relatively quiet sounds and C-weighting is used for detection of the peak SPLs (Parmanen, 2007) (Sun et al., 2016). Both A-weighting and C-weighting were developed to mimic the frequency responses of the human auditory system (Walworth, 1967). A-weighting was designed to be the best predictor for the ear's sensitivity to tones at low SPLs, while C-weighting was designed to follow the frequency sensitivity of the human ear at high SPLs. Therefore, the C-weighting function has a better estimation of the auditory system's response to high level sounds than the A-weighting (in terms of the magnitude perspective) (Houser et al., 2017).

A-weighting function, *AW(f)*, and C-weighting function, *CW(f)*, can be expressed as follows (Havelock, Kuwano, & Vorländer, 2008)

$$AW(f) = K_A \frac{\left(\frac{f}{f_1}\right)^2}{1+\left(\frac{f}{f_1}\right)^2} \frac{\left(\frac{f}{f_1}\right)}{\sqrt{1+\left(\frac{f}{f_2}\right)^2}} \frac{\left(\frac{f}{f_3}\right)}{\sqrt{1+\left(\frac{f}{f_3}\right)^2}} \frac{1}{1+\left(\frac{f}{f_4}\right)^2} \quad (1)$$

$$CW(f) = K_C \frac{\left(\frac{f}{f_1}\right)^2}{1+\left(\frac{f}{f_1}\right)^2} \frac{1}{1+\left(\frac{f}{f_4}\right)^2} \quad (2)$$

where K_A, K_C, f_1, f_2, f_3 and f_4 are constants given by approximate values: K_A = 1.258905, K_C = 1.007152, f_1= 20.60 Hz, f_2= 107.7 Hz, f_3 = 737.9 Hz, f_4 = 12194 Hz. The A-weighting and C-weighting are defined to have a unity gain at 1 kHz.

Figure 1 shows the frequency response of the A-weighted and the C-weighted filters. The A-weighted filter shows reduction at low frequencies (less

than 400 Hz), while the C-weighted filter is quite flat and has a very broad bandwidth (Havelock et al., 2008). Due to their abbreviated form, both A-weighted and C-weighted noise metrics have limitations on accurate assessment of a complex noise. Therefore, it is necessary and meaningful to develop new noise metrics, which can be used for more accurate assessment of the auditory risk for high-level complex noise (Dunn, Davis, Merry, & Franks, 1991) (Steele, 2001).

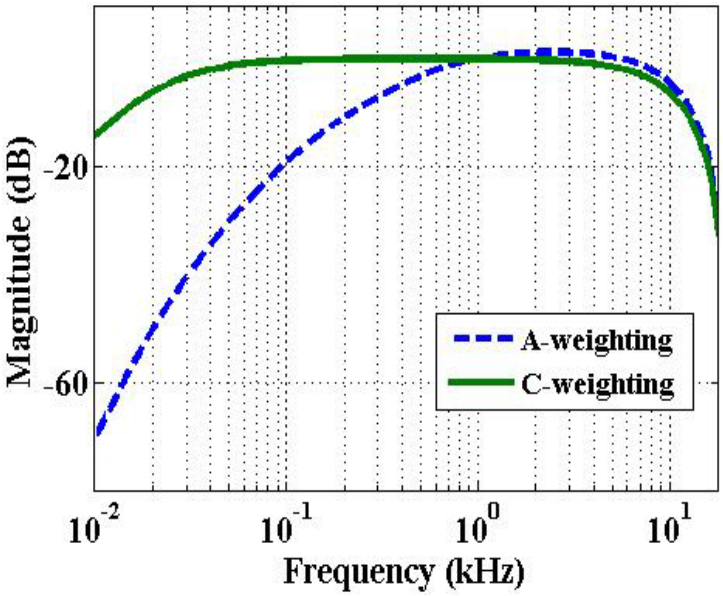

Figure 1. Frequency response of A-weighted and C-weighted filters.

2.2 Adaptive weighting (F-weighting)

We have proposed an adaptive weighting (F-weighting) which is based on the idea of blending the two standard weighting functions (*i.e.*, A-weighting and C-weighting) (Sun et al., 2016). In F-weighting, the sound pressure $P_{feq}(t)$ can be calculated as (Sun et al., 2016)

$$P_{feq}(t) = \alpha_{A,T}\left(AW(t) * P(t)\right) + \alpha_{C,T}\left(CW(t) * P(t)\right) \quad (3)$$

where *AW(t)* and *CW(t)* refer to A-weighed and C-weighted filters, respectively, '*' represents the convolution calculation. The parameters $\alpha_{A,T}$ and $\alpha_{C,T}$ are given by (Sun et al., 2016)

$$\alpha_{A,T} = exp(\beta K_T O_T)\frac{1}{|ln(O_T)|+1} \quad (4)$$

$$\alpha_{C,T} = exp(\beta K_T O_T)\frac{ln(O_T)|}{|ln(O_T)|+1} \quad (5)$$

where K_T is the kurtosis and O_T is the oscillation coefficient. β is a positive constant used to let the amplification component (*i.e.*, $exp(\beta K_T O_T)$) equal to one approximately in the case of Gaussian noise.

The kurtosis can be defined as the standardized fourth moment about the mean of the data (DeCarlo, 1997):

$$K_T = \frac{E[(x-\mu)^4]}{(E[(x-\mu)^2])^2} = \frac{\mu_4}{\sigma^4} \tag{6}$$

where E represents the expectation operator, μ represents the mean of x, μ_4 represents the fourth moment about the mean, and σ represents the standard deviation. A large kurtosis value implies more impulsive components in the noise (Qiu, Hamernik, & Davis, 2006) (Qiu, Hamernik, & Davis, 2013).

Another parameter, oscillation coefficient O_T, can be defined as (Hamila, Astola, Cheikh, Gabbouj, & Renfors, 1999)

$$O_T = \frac{\sum_{n=2}^{n-1} |(x_n - x_{n-1})(x_n + x_{n-1})|}{\sum_{n=2}^{n-1} x_n^2} \tag{7}$$

The oscillation coefficient is used to calculate the energy density distribution of the complex noise. O_T is relevant to the local transition level and the frequency of the noise signal. The product of the differential values in the O_T formula reflects the local transitions' strength of the noise signal.

2.3 Auditory fatigue model

In our previous study, we have developed an auditory fatigue model, complex velocity level (CVL) model, to predict gradually developing hearing loss (Sun, Qin, & Campbell, 2015). The CVL model combines an auditory filter which can obtain the velocities distributions on basilar membrane (BM) in cochlea, and a fatigue theory which is based on the Miner rule to calculate hearing loss associated with BM velocity.

2.3.1 Outer ear and middle ear transfer function

The mammalian ear consists of three parts: outer ear, middle ear, and inner ear. The primary path for the environmental sound to the inner ear is through the coupled motion of tympanic membrane (TM), ossicles, and stapes footplate. The main function of the outer ear and the middle ear is to gather sound energy into the inner ear. The outer ear consists of an ear canal, concha, and pinna flange. The middle ear consists of tympanic membrane, middle-ear air spaces, Eustachian tube,

and ossicles. The middle ear acts like an impedance-matching device that extracts acoustic energy from a stimulus and transmits it to the inner ear (Ruggero, Rich, Robles, & Shivapuja, 1990) (Slama, Ravicz, & Rosowski, 2010).

Figure 2 shows the transfer function for the outer ear and the middle ear of a chinchilla (Vrettakos, Dear, & Saunders, 1988). The transfer function of an outer ear has higher gain in mid-range frequencies (1000 – 8000 kHz). The transfer function of a middle ear is characterized by stapes velocity transfer function (SVTF), which is defined as the ratio between the linear velocity of the stapes and the sound pressure near TM in the ear canal (Slama et al., 2010).

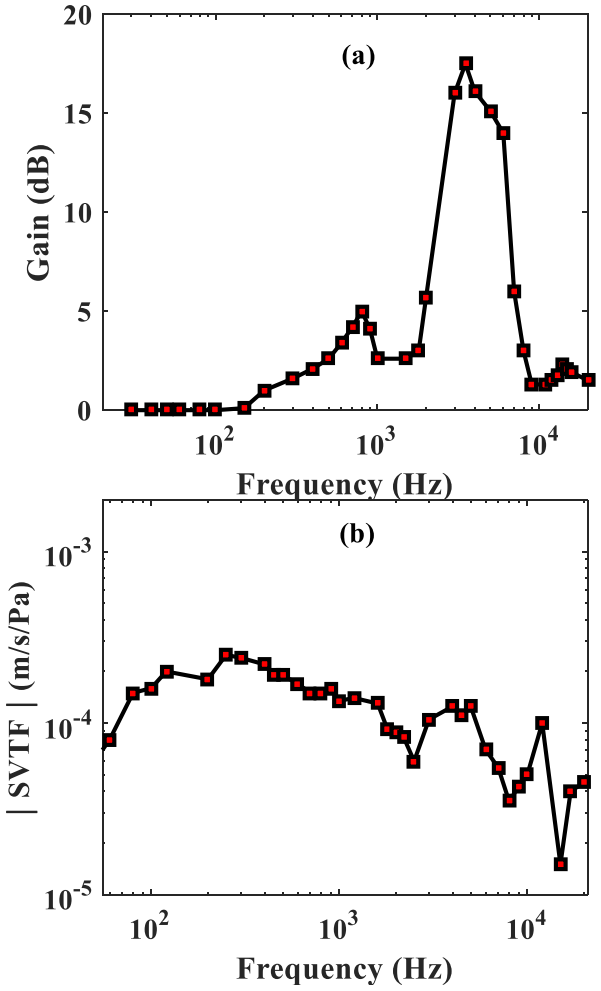

Figure 2. The transfer function of (a) the outer ear, and (b) the middle ear of chinchilla (Rosowski, 1991).

2.3.2 Inner ear model

The cochlea in an inner ear can be considered as a two-chambered, fluid-filled box with rigid side walls (Price & Kalb, 1991). The motion of the stapes produces pressure within the cochlea vestibule. The stimulus sound can be transferred as vibrations on the BM (Rhode & Cooper, 1996). In this study, the triple-path nonlinear (TRNL) filter (Lopez-Najera, Meddis, & Lopez-Poveda, 2005) was applied to obtain the BM responses along the cochlea partitions. Figure 3 shows the structure of the TRNL filter, in which the input is the middle ear stapes velocity and the output represents the velocity of the BM of a particular location at the cochlea partitions.

The TRNL filter consists of three parallel independent paths. The linear path contains a gain /attenuation factor, a bandpass function, and a low pass function in a cascade. The nonlinear path is a cascade combination of the 1st bandpass function, a compression function, the 2nd bandpass function, and a low pass function (Meddis, O'Mard, & Lopez-Poveda, 2001). Each individual bandpass function contains a cascade of two or more gammatone filters (Hartmann, 1997) with unit gain at the center frequency (CF). The third path is used to allow modeling of the amplitude and the phase plateaus at high frequency observed in the BM responses (Robles & Ruggero, 2001) (Lopez-Najera et al., 2005). Moreover, the compressive function shape in the nonlinear path is derived from the animal data, and it is defined as (Meddis et al., 2001)

$$y[t] = SIGN\ (x[t]) \times MIN\ (a|x[t]|, b|x[t]|^c) \qquad (8)$$

where $x[t]$ is the output from the first bandpass function in the nonlinear path. $y[t]$ represents the output of the compression function. a, b, and c are models parameters as summarized in Table 1.

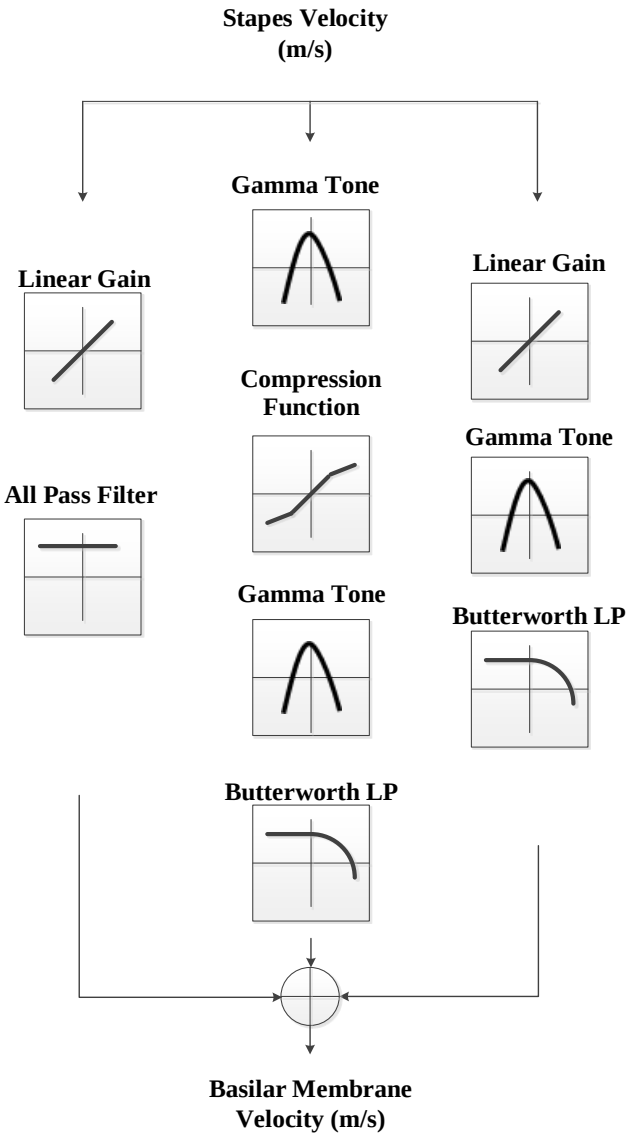

Figure 3. Schematic diagram of the TRNL filter, in which the input is the middle ear stapes velocities and the output is the velocity of the BM (Lopez-Najera et al., 2005) (Sun & Qin, 2016).

Table 1 - TRNL filter parameters used to simulate the chinchilla inner ear (Lopez-Najera et al., 2005) (Sun & Qin, 2016).

Simulated preparation	0.8 kHz	5.5 kHz	7.25 kHz	9.75 kHz	10 kHz	12 kHz	14 kHz
Linear							
GT cascade	5	5	5	5	5	5	5
LP cascade	7	7	7	7	7	7	7
CF_{lin}	750	5000	7400	9000	9000	11000	13000
BW_{lin}	450	3000	2500	3000	3500	5000	4000
LP_{lin}	750	6000	7400	9000	8800	12000	13500
Gain, g	500	190	3000	300	500	500	350
Nonlinear							
GT cascade	3	3	3	3	3	3	3
LP cascade	4	4	4	4	4	4	4
CF_{lin}	730	5850	7800	9800	10000	12000	15000
BW_{lin}	350	1800	2275	1650	1800	2000	3200
LP_{nl}	730	5850	7800	9800	10000	12000	15000
Gain, a	850	3000	15000	9000	15000	22500	3000
Gain, b	0.03	0.04	0.06	0.05	0.06	0.07	0.045
Exponent, c	0.25	0.25	0.25	0.25	0.25	0.25	0.25
Linear all-pass							
Gain, K	10	0.4	20	1	2	20	20

2.3.3 Complex velocity level (CVL) fatigue model

Sun *et al.* (Sun et al., 2015) proposed a complex velocity level (CVL) fatigue model based on the Miner's rule to calculate the noise induced cumulative hazard. The Miner's rule has been used to predict the materials' high-cycle fatigue life. The CVL model takes into account the amplitude transition and the mean value of the BM velocities that is correlated with hearing loss. The instantaneous hearing fatigue in a single BM vibration cycle at Δt can be described by (Sun et al., 2015)

$$H_{V(t),\Delta t} = \frac{\int_{\Delta t} V(t) dN(t)}{H_o} = \frac{\sum_j |V_j| . N_j}{H_o} \qquad (9)$$

where $V(t)$ is the BM velocities which are regarded as a complex stress. $N(t)$ is the corresponding failure cycle at time *t*. The discrete form refers to the *j*th category of the loads. H_o refers to the hearing loss at the equivalent rectangular band (ERB) with 1 kHz CF.

In real life, occupational noise is considered a complex load. The BM velocities can be demonstrated as a complex distribution. The hearing loss $H_{i,CVL}$ of the complex input loads (*i.e.*, the velocities of BM) is the integration of different types of the inputs along the time axis as follows (Sun et al., 2015)

$$H_{i,CVL} = \sum_{j \subset k} N_j . |V_{amplitude}(i,j) . V_{mean}(i,j)| \quad (10)$$

where k is the load categories total number with jth velocity type. i is the ERB band.

Thus, the CVL in the ERB band i can be represented by (Sun et al., 2015)

$$L_{i,CVL} = 10\, log_{10}\ \frac{\sum {H^2}_{i,CVL}}{{H^2}_o} \quad (11)$$

Where $L_{i,CVL}$ is the hearing loss metric log scale at the ith ERB.

2.4 Chinchilla noise exposure data

Chinchilla noise exposure data is used to evaluate the performances of the five noise metrics, including F-weighted SPL L_{Feq}, the CVL model based SPL L_{CVL}, and the three conventional noise metrics (*i.e.*, L_{eq}, L_{Aeq} and L_{Ceq}). The noise exposure data provided by a research group at State University of New York at Plattsburgh contains 263 chinchillas divided into 22 groups. Each group contained 9–16 chinchillas. Animals were exposed for five successive days to a certain noise for 24 hours per day. The 22 noise samples include 3 Gaussian noises (90, 95, and 100 dBA), and 19 complex noises (one sample at 95 dBA, two samples at 90 dBA, and 16 samples at 100 dBA). The hearing threshold level was measured at 0.5, 1, 2, 4, 8, and 16 kHz for each animal from the auditory evoked potential (AEP) before the exposure, daily, and 30 days after noise exposure. Permanent threshold shift (PTS) is defined as the permanent hearing loss measured 30 days after the noise exposure, and temporary threshold shift (TTS) refers to temporary hearing loss measured immediately after the noise exposure. Both PTS and TTS in 0.5, 1, 2, 4, 8, and 16 kHz octave bands were calculated based on the AEP data (as shown in Table 2). The noise data and the experimental protocols with detailed descriptions are available in several previous publications (Hamernik, Patterson, Turrentine, & Ahroon, 1989) (Hamernik, Qiu, & Davis, 2003a) (Hamernik et al., 2007). Table 2 summarized the PTS and the TTS values of each animal group for each octave band at center frequency 0.5, 1, 2, 4, 8, and 16 kHz.

Moreover, total effective hearing loss PTS_{5124} and TTS_{5124} can be calculated as the average of the PTS and TTS values at 0.5, 1, 2, and 4 kHz (Goley et al., 2011)

$$PTS_{5124} = (PTS_{0.5} + PTS_1 + PTS_2 + PTS_4)/4 \quad (12)$$

$$TTS_{5124} = (TTS_{0.5} + TTS_1 + TTS_2 + TTS_4)/4 \quad (13)$$

where $PTS_{0.5}, PTS_1, PTS_2$, and PTS_4 are the PTS values measured at 0.5, 1, 2, and 4 kHz respectively. $TTS_{0.5}, TTS_1, TTS_2$, and TTS_4 are TTS values measured at 0.5, 1, 2, and 4 kHz respectively.

Table 2 – PTS and TTS values of chinchillas of each group measure at six octave bands with center frequency at 0.5,1, 2, 4, 8, and 16 kHz.

Animal group index	PTS(dB)						TTS(dB)					
	0.5 kHz	1 kHz	2 kHz	4 kHz	8 kHz	16 kHz	0.5 kHz	1 kHz	2 kHz	4 kHz	8 kHz	16 kHz
G-44	17.1	26.2	39.4	42.9	46.5	43.7	58.6	70.1	79.3	85.4	85.8	70.6
G-49	22.1	34.3	47.2	54.6	46.8	47.2	62.6	75.3	77.6	86.5	79.9	70.6
G-50	7.7	10.1	8.0	15.8	14.1	17.7	37.2	57.6	63.4	76.1	79.8	69.2
G-51	15.7	19.5	29.0	24.3	27.8	25.1	59.7	63.9	73.2	75.9	81.9	67.9
G-52	18.5	24.5	36.8	32.9	28.3	23.3	63.9	72.4	76.4	81.2	80.1	69.6
G-53	19.0	24.4	34.5	31.7	29.9	28.1	59.4	68.0	77.4	85.0	84.3	69.0
G-54	16.2	18.5	29.9	31.4	25.4	29.1	55.7	65.3	75.6	82.5	80.0	66.3
G-55	18.8	21.7	36.5	46.8	60.1	47.5	67.1	74.1	76.2	82.3	80.3	68.8
G-60	20.7	27.8	34.1	34.1	29.3	27.8	59.3	68.4	70.8	75.7	75.9	65.2
G-61	2.6	5.0	10.0	20.5	18.2	24.0	36.1	45.6	50.4	74.4	80.4	72.0
G-63	25.4	31.4	43.8	36.2	32.3	28.9	63.4	69.8	76.2	76.4	73.4	65.0
G-64	15.8	17.4	24.7	22.1	19.0	13.5	60.0	66.3	73.8	79.4	73.9	67.1
G-65	17.2	14.4	25.0	39.6	49.5	48.3	62.5	62.8	68.1	74.4	75.8	70.7
G-66	7.5	9.3	19.2	32.9	44.8	36.2	49.4	58.9	70.0	82.9	76.1	70.4
G-68	12.9	13.9	21.7	39.7	47.3	47.3	65.9	69.2	71.1	81.1	75.0	73.3
G-69	4.8	10.9	9.3	11.3	5.5	8.0	28.8	47.4	48.8	49.3	47.8	50.1
G-70	12.1	17.9	27.6	43.2	30.4	35.1	59.9	69.9	75.0	84.8	76.8	71.0
G-47	0.3	-0.3	3.3	1.9	7.5	6.7	22.4	34.3	41.6	60.9	68.7	60.7
G-48	3.0	6.8	9.4	5.4	11.2	10.8	26.9	35.9	37.6	41.5	58.0	63.9
G-56	2.9	1.7	4.5	8.9	14.7	8.9	29.5	30.5	29.2	39.3	52.0	50.9
G-57	6.8	5.8	6.7	16.7	23.3	18.9	35.5	41.4	52.1	66.4	71.8	66.0
G-58	7.8	8.8	18.9	17.5	15.0	17.9	44.5	50.3	59.1	62.1	62.1	63.6

3 RESULTS AND DISCUSSIONS

The linear regression analysis of the five noise metrics (*i.e.*, L_{eq}, L_{Aeq}, L_{Ceq}, L_{Feq}, and L_{CVL}), and hearing loss indicators (PTS and TTS values at various octave bands) were conducted using all 22 groups of animal experimental data. The coefficient of determination (r^2) is used to evaluate the performance of each metric. The r^2 value indicates the correlation between the metrics and the hearing loss indicators. When the value of the r^2=1, it indicates a perfect correlation and when r^2=0 it means there is no correlation between noise metrics and hearing loss data.

Table 3 summarizes the r^2 values between the hearing loss indicators (PTS and TTS at six octave bands centered at 0.5, 1, 2, 4, 8, and 16 kHz), and the five noise metrics (L_{eq}, L_{Aeq}, L_{Ceq}, L_{Feq}, and L_{CVL}). The results show that L_{CVL} achieves the best correlation with the PTS at 0.5, 2, 4, 8, and 16 kHz. For TTS, L_{CVL} has the best correlation at 0.5, 2, 8, and 16 kHz. The higher correlation between the hearing loss and the CVL model indicates that it can be used to predict NIHL accurately.

Table 3 – Comparison of the regression analysis results of the two hearing loss indices represented by PTS and TTS with all metrics (*i.e.*, L_{eq}, L_{Aeq}, L_{Ceq}, L_{Feq}, and L_{CVL}) at six octave bands centered at 0.5, 1, 2, 4, 8, and 16 kHz.

	r^2											
	PTS						*TTS*					
Metric	0.5 kHz	1 kHz	2 kHz	4 kHz	8 kHz	16 kHz	0.5 kHz	1 kHz	2 kHz	4 kHz	8 kHz	16 kHz
L_{eq}	0.13	0.59	0.21	0.65	0.3	0.13	0.33	0.67	0.37	**0.8**	0.51	0.53
L_{Aeq}	0.16	**0.61**	0.21	0.65	0.33	0.17	0.37	**0.69**	0.37	**0.8**	0.48	0.55
LC_{eq}	0.13	0.59	0.21	0.65	0.33	0.17	0.33	0.67	0.37	**0.8**	0.48	0.55
LF_{eq}	0.2	0.58	0.24	0.62	0.33	0.18	0.44	0.66	0.41	0.72	0.47	0.53
L_{CVL}	**0.24**	0.4	**0.62**	**0.7**	**0.52**	**0.54**	**0.56**	0.64	**0.75**	0.77	**0.6**	**0.56**

Additionally, Figure 4 shows the correlation analysis between the three metrics (L_{Aeq}, L_{Feq}, and L_{CVL}) and hearing loss indicators (*i.e.*, PTS and TTS values at 0.5, 1, 2, 4, 8, and 16 kHz octave bands). The lines in the figure represent the fitting results of the distributions of the symbols. The highest correlation between L_{Feq} and both of the hearing loss indicators happens at 4 kHz octave band. Similar

to the F-weighting, the CVL model shows the highest correlation with both PTS and TTS at 4 kHz.

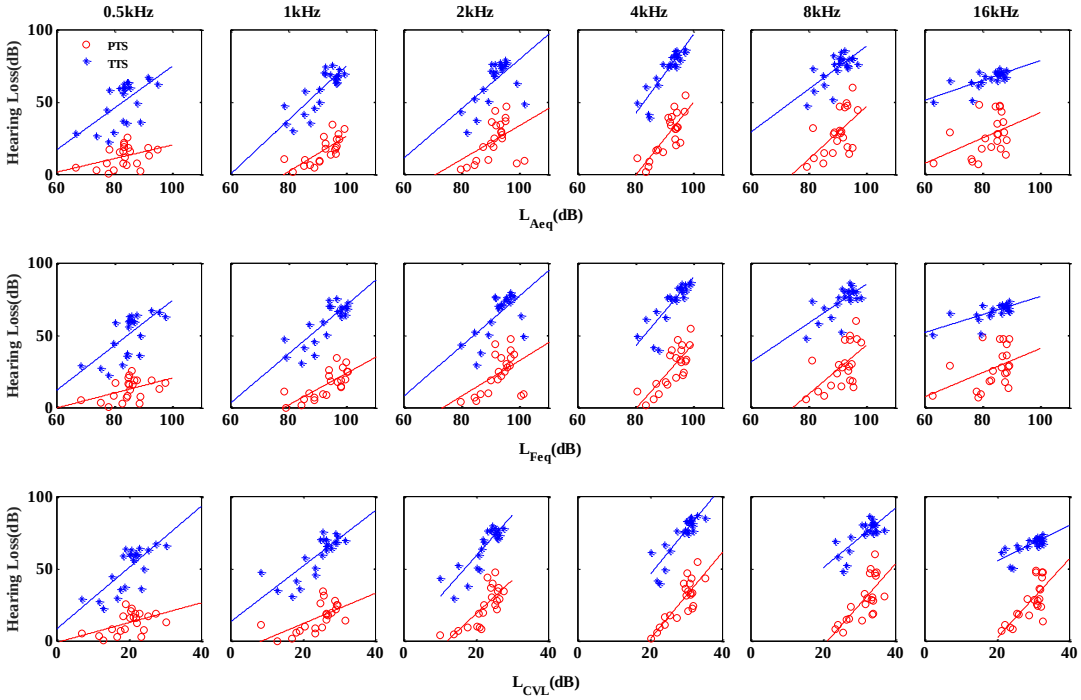

Figure 4. Scatting plots and fitting lines between three noise metrics (L_{Aeq}, L_{Feq}, and L_{CVL}) and hearing loss indicators (PTS and TTS) at six octave bands with center frequency at 0.5, 1, 2, 4, 8, and 16 kHz. The red color represents PTS and the blue color represents TTS.

Moreover, the linear regression analysis of the five noise metrics (L_{eq}, L_{Aeq}, L_{Ceq}, L_{Feq}, and L_{CVL}) and the effective hearing loss indicators (TTS_{5124} and PTS_{5124}) are conducted. The correlations between the five noise metrics (L_{eq}, L_{Aeq}, L_{Ceq}, L_{Feq}, and L_{CVL}) and the effective total hearing loss PTS_{5124} and TTS_{5124} are summarized in Table 4. The results show that the CVL fatigue model achieves the highest r^2 values for both PTS_{5124} (r^2=0.61) and TTS_{5124} (r^2=0.84) among all of the five noise metrics. It indicates that the CVL model is more accurate than the other four metrics for assessment of NIHL.

F-weighting also has higher correlations with PTS_{5124} than the other three conventional noise metrics (L_{eq}, L_{Aeq}, and L_{Ceq}). For TTS_{5124}, L_{Feq} achieves same r^2 with L_{Ceq}, and both are higher than L_{eq} and L_{Aeq}. Therefore, the F-weighting metric can be more accurate for assessment of NIHL compared with the L_{eq}, L_{Aeq}, and L_{Ceq}.

Table 4 – Regression analysis results of the five noise metrics (L_{eq}, L_{Aeq}, L_{Ceq}, L_{Feq}, and L_{CVL}) and effective hearing loss indicators PTS_{5124} and TTS_{5124}.

	r^2	
Metric	PTS_{5124}	TTS_{5124}
L_{eq}	0.44	0.69
L_{Aeq}	0.50	0.68
L_{Ceq}	0.50	0.71
L_{Feq}	0.55	0.71
L_{CVL}	**0.61**	**0.84**

Figure 5 shows scatting plots and fitting lines of linear regression analysis between the five noise metrics and the effective hearing loss indictors. The fitting lines show a positive proportion between the five noise metrics and effective hearing loss indictors (PTS_{5124} and TTS_{5124}). The positive relationship indicates that these metrics can be used to evaluate the hearing loss effectively. The results are consistent with Table 4.

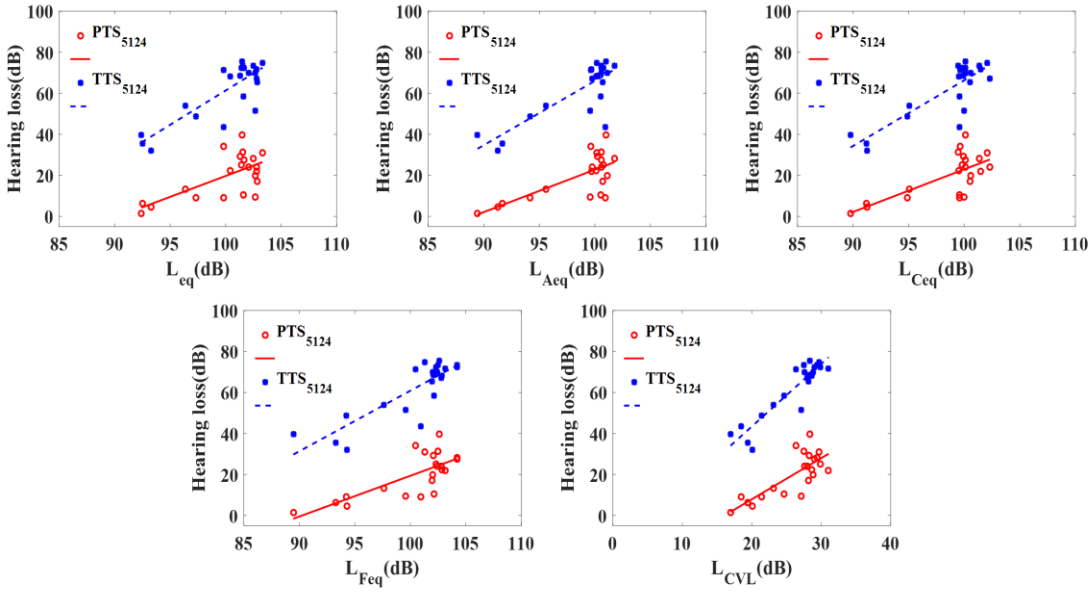

Figure 5. Scatting plots and fitting lines of five noise metrics (L_{eq}, L_{Aeq}, L_{Ceq}, L_{Feq}, and L_{CVL}) and effective hearing loss indicators (PTS_{5124} and TTS_{5124}). The red color represents PTS_{5124} and the blue color represents TTS_{5124}.

4 CONCLUSIONS

In this study, we compared the performances of two newly developed noise models (*i.e.*, F-weighting and CVL fatigue model) with the conventional noise metrics (*i.e.*, L_{eq}, L_{Aeq}, and L_{Ceq}) using animal noise exposure data. Linear regression analysis was used to evaluate the correlations between the five noise metrics (L_{eq}, L_{Aeq}, L_{Ceq}, L_{Feq}, and L_{CVL}) and the hearing loss indicators (PTS and TTS centered at 0.5, 1, 2, 4, 8, and 16 kHz octave bands). Moreover, to evaluate the effective hearing loss, the linear regression analysis was conducted between the five noise metrics and the effective hearing loss (PTS_{5124} and TTS_{5124}). The results show that the CVL fatigue model demonstrates the highest correlations with the hearing loss indicators and the effective hearing loss among the five noise metrics. The F-weighting also achieves higher correlations with the hearing loss data compared with the three conventional noise metrics L_{eq}, L_{Aeq}, and L_{Ceq}. It indicates that both developed metrics (*i.e.*, CVL model and F-weighting) can predict the NIHL better than the conventional EEH based noise metrics in the current noise measurement standard. The F-weighting and CVL fatigue model can be applied to assess occupational noise induced hearing loss in various industrial and military applications.

5 REFERENCES

AMSC, N., & HFAC, A. A. DEPARTMENT OF DEFENSE DESIGN CRITERIA STANDARD. *Signal, 44*(5.3), 4.

Azizi, M. H. (2010). Occupational noise-induced hearing loss. *The international journal of occupational and environmental medicine, 1*(3 July).

Blakeslee, E., Hynson, K., Hamernik, R., & Henderson, D. (1977). Interaction of spectrally-mismatched continuous and impulse-noise exposures in the chinchilla. *The Journal of the Acoustical Society of America, 61*(S1), S59-S59.

DeCarlo, L. T. (1997). On the meaning and use of kurtosis. *Psychological methods, 2*(3), 292.

Dunn, D. E., Davis, R. R., Merry, C. J., & Franks, J. R. (1991). Hearing loss in the chinchilla from impact and continuous noise exposure. *The Journal of the Acoustical Society of America, 90*(4), 1979-1985.

Goley, G. S., Song, W. J., & Kim, J. H. (2011). Kurtosis corrected sound pressure level as a noise metric for risk assessment of occupational noises. *The Journal of the Acoustical Society of America, 129*(3), 1475-1481.

Hamernik, R. P., Ahroon, W. A., Davis, R. I., & Lei, S. F. (1994). Hearing threshold shifts from repeated 6-h daily exposure to impact noise. *The Journal of the Acoustical Society of America, 95*(1), 444-453.

Hamernik, R. P., Henderson, D., Crossley, J. J., & Salvi, R. J. (1974). Interaction of continuous and impulse noise: audiometric and histological effects. *The Journal of the Acoustical Society of America, 55*(1), 117-121.

Hamernik, R. P., Patterson, J. H., Turrentine, G. A., & Ahroon, W. A. (1989). The quantitative relation between sensory cell loss and hearing thresholds. *Hearing research, 38*(3), 199-211.

Hamernik, R. P., & Qiu, W. (2000). Correlations among evoked potential thresholds, distortion product otoacoustic emissions and hair cell loss following various noise exposures in the chinchilla. *Hearing research, 150*(1), 245-257.

Hamernik, R. P., Qiu, W., & Davis, B. (2003a). Cochlear toughening, protection, and potentiation of noise-induced trauma by non-Gaussian noise. *The Journal of the Acoustical Society of America, 113*(2), 969-976.

Hamernik, R. P., Qiu, W., & Davis, B. (2003b). The effects of the amplitude distribution of equal energy exposures on noise-induced hearing loss: The kurtosis metric. *The Journal of the Acoustical Society of America, 114*(1), 386-395.

Hamernik, R. P., Qiu, W., & Davis, B. (2007). Hearing loss from interrupted, intermittent, and time varying non-Gaussian noise exposure: The applicability of the equal energy hypothesis. *The Journal of the Acoustical Society of America, 122*(4), 2245-2254.

Hamila, R., Astola, J., Cheikh, F. A., Gabbouj, M., & Renfors, M. (1999). Teager energy and the ambiguity function. *IEEE Transactions on Signal Processing, 47*(1), 260-262.

Hartmann, W. M. (1997). *Signals, sound, and sensation*: Springer Science & Business Media.

Havelock, D., Kuwano, S., & Vorländer, M. (2008). *Handbook of signal processing in acoustics*: Springer Science & Business Media.

Health, U. D. o., & Services, H. (1998). Criteria for a Recommended Standard: Occupational Noise Exposure Revised Criteria. *Cincinnati, OH*, 1-122.

Henderson, D., & Hamernik, R. (1986). Impulse noise: critical review. *The Journal of the Acoustical Society of America, 80*(2), 569-584.

Houser, D. S., Yost, W., Burkard, R., Finneran, J. J., Reichmuth, C., & Mulsow, J. (2017). A review of the history, development and application of auditory weighting functions in humans and marine mammals. *The Journal of the Acoustical Society of America, 141*(3), 1371-1413.

Lopez-Najera, A., Meddis, R., & Lopez-Poveda, E. A. (2005). A computational algorithm for computing cochlear frequency selectivity: Further studies *Auditory Signal Processing* (pp. 14-20): Springer.

Meddis, R., O'Mard, L. P., & Lopez-Poveda, E. A. (2001). A computational algorithm for computing nonlinear auditory frequency selectivity. *The Journal of the Acoustical Society of America, 109*(6), 2852-2861.

Murphy, W. J., & Kardous, C. A. (2012). A case for using a-weighted equivalent energy as a damage risk criterion. *National Institute for Occupational Safety and Health, EPHB Report No*.

Parmanen, J. (2007). A-weighted sound pressure level as a loudness/annoyance indicator for environmental sounds–Could it be improved? *Applied Acoustics, 68*(1), 58-70.

Price, G. R. (2012). Impulse noise hazard: From theoretical understanding to engineering solutions. *Noise Control Engineering Journal, 60*(3), 301-312.

Price, G. R., & Kalb, J. T. (1991). Insights into hazard from intense impulses from a mathematical model of the ear. *The Journal of the Acoustical Society of America, 90*(1), 219-227.

Qin, J., & Sun, P. (2015). Applications and comparison of continuous wavelet transforms on analysis of a-wave impulse noise. *Archives of Acoustics, 40*(4), 503-512.

Qin, J., Sun, P., & Walker, J. (2014). *Measurement of field complex noise using a novel acoustic detection system.* Paper presented at the AUTOTESTCON, 2014 IEEE.

Qiu, W., Hamernik, R. P., & Davis, B. (2006). The kurtosis metric as an adjunct to energy in the prediction of trauma from continuous, nonGaussian noise exposures. *The Journal of the Acoustical Society of America, 120*(6), 3901-3906.

Qiu, W., Hamernik, R. P., & Davis, R. I. (2013). The value of a kurtosis metric in estimating the hazard to hearing of complex industrial noise exposures. *The Journal of the Acoustical Society of America, 133*(5), 2856-2866.

Rhode, W. S., & Cooper, N. P. (1996). Nonlinear mechanics in the apical turn of the chinchilla cochlea in vivo. *Aud. Neurosci, 3*(101), U121.

Robles, L., & Ruggero, M. A. (2001). Mechanics of the mammalian cochlea. *Physiological reviews, 81*(3), 1305-1352.

Rosowski, J. J. (1991). The effects of external-and middle-ear filtering on auditory threshold and noise-induced hearing loss. *The Journal of the Acoustical Society of America, 90*(1), 124-135.

Ruggero, M. A., Rich, N. C., Robles, L., & Shivapuja, B. G. (1990). Middle-ear response in the chinchilla and its relationship to mechanics at the base of the cochlea. *The Journal of the Acoustical Society of America, 87*(4), 1612-1629.

Slama, M. C., Ravicz, M. E., & Rosowski, J. J. (2010). Middle ear function and cochlear input impedance in chinchilla. *The Journal of the Acoustical Society of America, 127*(3), 1397-1410.

Sliwinska-Kowalska, M., & Davis, A. (2012). Noise-induced hearing loss. *Noise and Health, 14*(61), 274.

Smalt, C. J., Lacirignola, J., Davis, S. K., Calamia, P. T., & Collins, P. P. (2017). Noise dosimetry for tactical environments. *Hearing research, 349*, 42-54.

Smith, G. (1996). Noise? What noise? *Occupational health & safety (Waco, Tex.), 65*(3), 38-38.

Smoorenburg, G. F. (1980). *Damage Risk Criteria for Impulse Noise [microvorm]*: Institute for Perception, TNO.

Starck, J., & Pekkarinen, J. (1987). Industrial impulse noise: crest factor as an additional parameter in exposure measurements. *Applied Acoustics, 20*(4), 263-274.

Steele, C. (2001). A critical review of some traffic noise prediction models. *Applied Acoustics, 62*(3), 271-287.

Sun, Fox, D., Campbell, K., & Qin, J. (2017). Auditory fatigue model applications to predict noise induced hearing loss in human and chinchilla. *Applied Acoustics, 119*, 57-65.

Sun, & Qin, J. (2016, 24-27 Feb. 2016). *Auditory fatigue models for prediction of gradually developed noise induced hearing loss.* Paper presented at the 2016 IEEE-EMBS International Conference on Biomedical and Health Informatics (BHI).

Sun, Qin, J., & Campbell, K. (2015). Fatigue Modeling via Mammalian Auditory System for Prediction of Noise Induced Hearing Loss. *Computational and mathematical methods in medicine, 2015*.

Sun, Qin, J., & Qiu, W. (2016). Development and validation of a new adaptive weighting for auditory risk assessment of complex noise. *Applied Acoustics, 103*, 30-36.

Tak, S., Davis, R. R., & Calvert, G. M. (2009). Exposure to hazardous workplace noise and use of hearing protection devices among US workers—NHANES, 1999–2004. *American journal of industrial medicine, 52*(5), 358-371.

Vrettakos, P. A., Dear, S. P., & Saunders, J. C. (1988). Middle ear structure in the chinchilla: a quantitative study. *American journal of otolaryngology, 9*(2), 58-67.

Walworth, H. T. (1967). Guidelines for Noise Exposure Control: Intersociety Committee Report. *Journal of Occupational and Environmental Medicine, 9*(11), 571-575.

Wu, Q., & Qin, J. (2013). Effects of key parameters of impulse noise on prediction of the auditory hazard using AHAAH model. *International journal of computational biology and drug design, 6*(3), 210-220.

Zhu, X., Kim, J. H., Song, W. J., Murphy, W. J., & Song, S. (2009). Development of a noise metric for assessment of exposure risk to complex noises. *The Journal of the Acoustical Society of America, 126*(2), 703-712.